Electrodeposition Study on a Single-crystal Titanium Dioxide Electrode: Platinum on a Niobium-doped Titanium Dioxide(110) Electrode

Satoru Takakusagi, *[1] Takafumi Ogawa, [1] Hiromitsu Uehara, [1] Hiroko Ariga, [1] Ken-ichi Shimizu, [1]and Kiyotaka Asakura *[1]
[1]*Catalysis Research Center, Hokkaido University, Kita21 Nishi10, Kita-ku, Sapporo, Hokkaido, 001-0021*

(Received <Month> <Date>, <Year>; CL-<No>; E-mail: <insert corresponding e-mail address>)

Pt was successfully electrodeposited on a Nb-doped TiO_2(110) electrode from a solution of 1 mM K_2PtCl_4 + 50 mM H_2SO_4 using single-pulse chronoamperometry. The morphology of the deposited Pt nanoparticles was sensitive to the deposition potential and holding time. A novel method for the preparation of metal particles on a TiO_2 single-crystal surface in a controlled manner has been proposed.

Electrochemical metal deposition is widely used to prepare metal thin films, particles, and nanostructured materials on solid surfaces. Film thickness, particle size/shape, and morphology of the deposited metal can be controlled by adjusting and optimizing electrochemical conditions such as the electrode potential, holding time, and electrolyte. In contrast to electrochemical metal deposition on metal or semiconductor substrates, deposition on oxide surfaces has rarely been performed and has been limited only to oxide thin films formed on conductive substrates probably due to insufficient conductivity of oxide itself.[1-4] However, the deposition of metal on an oxide surface is important for applications such as oxide-supported metal catalysts, where the catalytic properties are largely dependent both on the metal particle size/shape and on the strength of the metal-support interaction.[5] Therefore, electrochemical metal deposition on an oxide surface could be a promising method to obtain well-controlled nanoparticles on oxide surfaces and it is important to reveal the deposition mechanism.

We selected the Nb-doped (0.05 wt%) TiO_2(110) surface as a model system because of its suitability for atomic-scale surface chemistry and its sufficient conductivity. Rutile TiO_2 single-crystal surfaces, particularly the (110) face,[6,7] are the most studied single-crystal oxide surfaces, of which atomically flat and Nb-doped conductive TiO_2(110) has recently become available.[8,9] The electrodeposition of Pt on the Nb-doped TiO_2(110) is investigated here using single-pulse chronoamperometry. To our knowledge, this is the first study of metal electrodeposition on a TiO_2 single-crystal surface. The effect of the electrode potential and holding time on the morphology of the electrodeposited Pt on the Nb-doped TiO_2(110) was examined, and we have found that the Pt nanoparticles with different aspect ratios (height/apparent diameter) can be prepared by choosing appropriate deposition conditions.

Figure 1 shows cyclic voltammograms (CVs) of a Nb-doped (0.05 wt%) TiO_2(110) electrode in 50 mM H_2SO_4 and in a solution of 1 mM K_2PtCl_4 + 50 mM H_2SO_4. In-Ga eutectic alloy was attached to the backside of the TiO_2(110) surface for ohmic contact and both electrolyte solutions were deoxygenated before the measurements. In the 50 mM H_2SO_4 solution, when the electrode potential was scanned in the negative direction, cathodic current started to flow at around

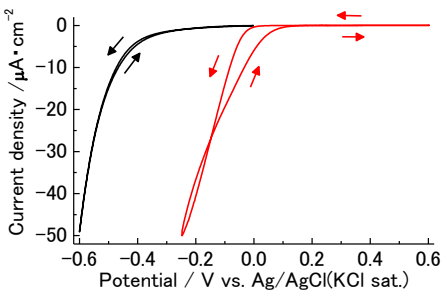

Figure 1. CVs of a Nb-doped TiO_2(110) electrode in 50 mM H_2SO_4 (black line) and in 1 mM K_2PtCl_4 + 50 mM H_2SO_4 solution (red line). Scan rate 10 mV/s.

-0.3 V due to the hydrogen evolution reaction (HER; $2H^+ + 2e^- \rightarrow H_2$). However, in 1 mM K_2PtCl_4 + 50 mM H_2SO_4 solution, the cathodic current began to flow at around 0 V according to the following reaction:

$$PtCl_4^{2-} + 2e^- \rightarrow Pt + 4Cl^- \quad (1)$$

Considering that the reversible potential for the reaction (1) in 1 mM $PtCl_4^{2-}$ was calculated to be 0.49 V vs. Ag/AgCl(KCl sat.), a large overpotential was required to initiate Pt deposition, probably due to the semiconductive properties of the Nb-doped TiO_2(110) electrode.

Figures 2(a) and (b) show tapping-mode AFM images of the Nb-doped TiO_2(110) surface after electrodeposition at -0.15 V for 1 and 10 s, respectively. The TiO_2(110) electrode was first immersed in the electrolyte solution at +0.58 V and stepped to -0.15 V. After holding the potential for 1s or 10 s, it was then stepped back to +0.58 V and the sample was removed from the solution. The electric charges passing across the electrode were 98 μC/cm^2 and 348 μC/cm^2 for deposition time 1s and 10 s, respectively. The Pt particles were homogeneously distributed on the surface in both cases. Histograms of the height and apparent diameter for the Pt nanoparticles in Figs. 2(a) and (b), which were determined by cross-sectional analysis in the images, are shown in Figs. 2(c) and (d), respectively. The apparent particle diameter is sometimes corrected by assuming an appropriate shape (hemisphere or sphere) both for deposited particles and the AFM tip; however, this was not performed, because in this study we observed Pt particles which have similar height but different diameter (different aspect ratios). Particles with a maximum size of ca. 24 nm in height and ca. 170 nm in apparent diameter were formed with a deposition time of 1 s, where the average particle height and apparent diameter were 13±7 nm and 111±43 nm, respectively. A longer deposition time (10 s) resulted in a more significant increase in height and height distribution than that in the apparent diameter and

corresponding distribution (average height: 35±18 nm, average apparent diameter: 102±37 nm). Note that there was no significant change in particle density with deposition for 1 s ((3.9±0.5)×10^8 /cm^2) and 10 s ((3.5±0.5)×10^8 /cm^2), which indicates that nucleation rate was much slower than the growth rate.

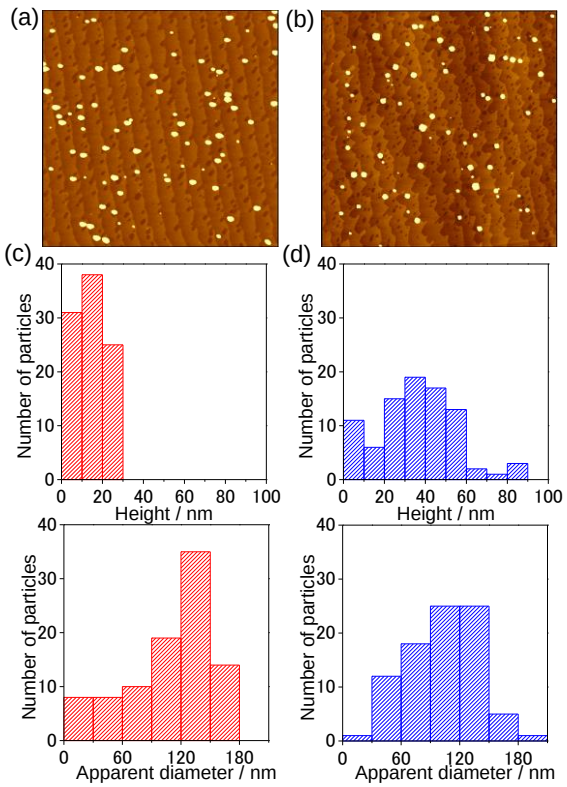

Figure 2. AFM images (5×5 μm^2) of the Nb-doped TiO_2(110) surface after electrodeposition at -0.15 V for (a) 1s and (b) 10 s. (c) and (d) are histgrams of apparent diameter and height of the Pt nanoparticles observed in (a) and (b), respectively

Figure 3 shows the particle height as a function of the apparent diameter for the Pt particles at deposition times of 1 and 10 s. The plots clearly indicate that vertical growth of the Pt particles is preferential over lateral growth when the deposition time is increased. This is probably due to more efficient electrodeposition on the predeposited Pt particles than on the TiO_2(110) surface due to the stronger interaction of the $PtCl_4^{2-}$ complex with the surfaces of Pt particles than with the TiO_2 substrate, even if the TiO_2(110) surface is activated as discussed later. Vertical (three-dimensional) growth of Pt nanoparticles was also reported for the electrochemical deposition of Pt on a semiconductor n-type Si(111) electrode.[10]

Figures 4(a) and (b) show AFM images of the Nb-doped TiO_2(110) surface after electrodeposition at a smaller overpotential (-0.05 V) for 1 and 10 s, respectively. The electric charges flowing across the electrode were 16 μC/cm^2 and 269 μC/cm^2 for deposition time 1s and 10 s, respectively. In Fig. 4(a), much smaller nanoparticles with narrower size distribution were obtained compared with those in Fig. 2(a) as indicated by the histograms in Fig. 4(c). The average particle height and apparent diameter were 1.5±0.6 nm and 20±4 nm,

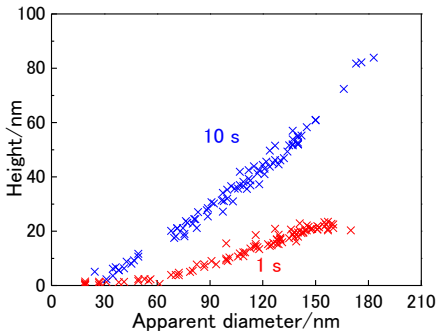

Figure 3. Plots of the particle height as a function of the apparent diameter for the Pt particles deposited at -0.15 V for 1s (red) and 10 s (blue).

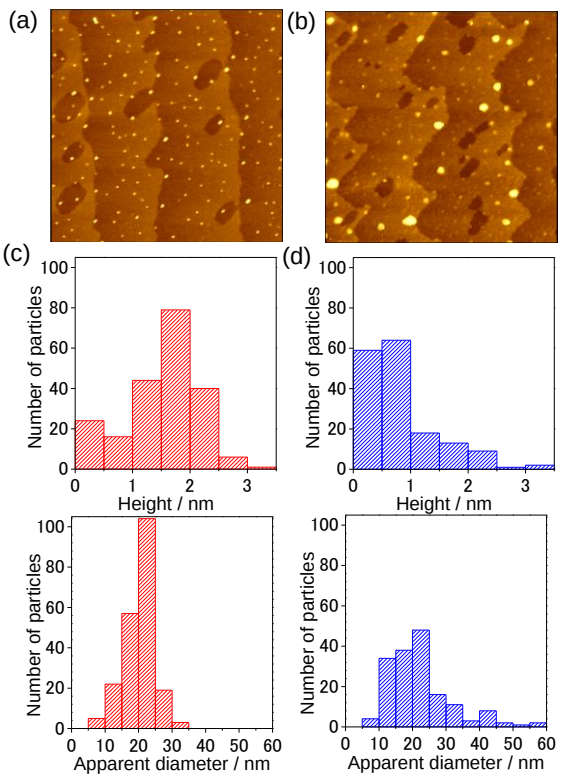

Figure 4. AFM images (1×1 μm^2) of the Nb-doped TiO_2(110) surface after electrodeposition at -0.05 V for (a) 1s and (b) 10 s. (c) and (d) are histgrams of apparent diameter and height of the Pt nanoparticles observed in (a) and (b), respectively.

respectively. The particle density was (9.9±0.8)×10^9 /cm^2, which was much larger than that obtained at -0.15 V in Fig. 2(a). Pt nanoparticles were formed on TiO_2 terrace surfaces and no selective deposition at the step edges was observed, which is similar to the results for evaporated Pt deposition on a TiO_2(110) surface in an ultra-high vacuum (UHV) environment.[11,12]

When the deposition time is increased to 10 s, the particle shape is significantly changed, as shown in the AFM image (Fig. 4(b)) and the corresponding histograms (Fig. 4(d)). The average particle height and apparent diameter were 0.8±0.6 nm and 22±9 nm, respectively, and the particle density was (8.9±0.8)×10^9 /cm^2. Note that the number of the

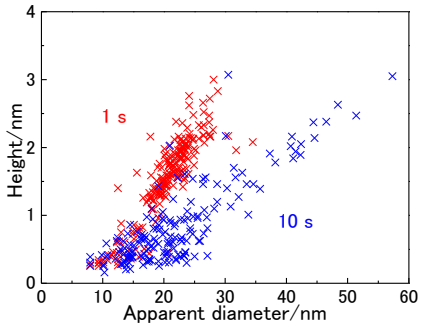

Figure 5. Plots of the particle height as a function of the apparent diameter for the Pt particles deposited at -0.05 V for 1s (red) and 10 s (blue).

particles with heights larger than 1.0 nm significantly decreased after electrodeposition for 10 s, while the number of the particles with apparent diameters larger than 30 nm increased, as shown in Figs. 4(c) and (d). The particle height as a function of apparent diameter presented in Figure 5 indicates that the number of flat-shaped particles increases and lateral growth is preferential over vertical growth. It is also noted in Fig.5 that for a deposition time of 1 s, most of the deposited Pt particles (99%) were in the range of <3 nm in height with apparent diameters of <30 nm, while for a deposition time of 10 s, 74% of the particles were <1 nm in height with apparent diameters of <30 nm. Considering the results obtained at -0.05 V, the deposited Pt atoms were mobile and redispersed onto the TiO_2 surface during the deposition process, and the Pt particles changed their shape form three-dimensional to flat two-dimensional one.

The origin of the change in particle shape during the electrodeposition process could be due to the delayed enhancement of the interaction between Pt and TiO_2 at -0.05 V. The interaction between Pt atoms and TiO_2(110) may not be so large at a deposition time of 1 s, so that the deposited Pt atoms could migrate on the surface to find other Pt atoms to form nuclei or small particles. Because of the small size of nuclei or small particles, they were not yet stable, and the Pt atoms forming them could move to make further contact with the TiO_2 surface when the deposition time is increased and the interaction between Pt and TiO_2 becomes enhanced, resulting in the particle shape change from three-dimensional to two-dimensional morphology. Adsorbed hydrogen on the Pt surface would facilitate migration of the Pt atoms by weakening the Pt-Pt bonds.[13,14] We speculate that hydrogen (or proton) spillover from the Pt particles to form OH groups on the adjacent TiO_2 sites could be a possible reason for the delayed enhancement of Pt-TiO_2 interaction. For example, hydrogen spillover from Pt nanoparticles onto a fluorine-doped tin oxide (FTO) surface under an electrochemical environment has been recently reported.[15] Pt might produce more OH groups on the TiO_2(110) than the bare TiO_2(110) without Pt due to the catalytic effect of Pt under the applied potential, and local density of OH groups around the deposited Pt particles would increase. OH groups on oxide surfaces have a stronger interaction with metal species and can act as metal nucleation sites,[16-18] which would promote the change in particle shape from three-dimensional to two-dimensional one. A similar situation should have been observed for Pt deposition at -0.15 V; however, the growth of Pt nanoparticles was much faster at -0.15 V to form large stable Pt particles before the formation of a sufficient number of OH groups on the TiO_2(110) surface. In situ AFM measurements of the Pt deposition process are presently in progress to reveal the detailed growth mechanism at -0.05 V.

In conclusion, Pt was successfully electrodeposited on a Nb-doped TiO_2(110) surface and the structure of the deposited Pt nanoparticles was examined using AFM. The height and apparent diameter distributions of the Pt nanoparticles changed significantly with the deposition potential and time. Vertical growth of Pt nanoparticles was preferential over lateral growth at -0.15 V, whereas the shape of the deposited Pt particles changed from three- to two-dimensional one at -0.05 V when the deposition time was increased. Pt nanoparticles with different aspect ratios (height/apparent diameter) can thus be prepared by the selection of appropriate deposition conditions, as shown in Figs. 3 and 5. A novel method for the preparation of metal nanoparticles on a TiO_2 single-crystal surface in a controlled manner has been proposed.

This work was financially supported by a Grant-in-Aid for Scientific Research on Innovative Areas "Nano Informatics" (No. 25106010) from JSPS and NEDO (Demonstrative Research on Solid Oxide Fuel Cells/Fundamental Technologies Development/Analysis of Structure, Reactions, and Material Transfer of MEA Materials).

References

1 R.E. Rettew, N.K. Allam, F.M. Alamgir, F. M., *ACS Appl. Mater. Interfaces*, **2011**, *3*, 147.
2 C.-S. Chen, F.-M. Pan, *Appl. Catal., B: Environ*., **2009**, *91*, 663.
3 E. Formo, E. Lee, D. Campbell, Y. Xia, *Nano Lett.*, **2008**, *8*, 668.
4 M.B. Vukmirovic, P. Liu, J.T. Muckerman, R.R. Adzic, *J. Phys. Chem. C*, **2007**, *111*, 15306.
5 A.M. Ruppert, B.M. Weckhuysen, in Handbook of Heterogeneous Catalysis, eds. G. Ertl, H. Knozinger, F. Schuth, J. Weitkamp, 2008; p 1178.
6 C.L. Pang, R. Lindsay, G. Thornton, *Chem. Rev.*, **2013**, *113*, 3887
7 U. Diebold, *Surf. Sci. Rep.*, **2003**, *48*, 53.
8 Y. Yamamoto, K. Nakajima, T. Ohsawa, Y. Matsumoto, H. Konuma, *Jpn. J. Appl. Phys.*, **2005**, *44*, L511.
9 R. Nakamura, N. Ohashi, A.Imanishi, T. Osawa, Y. Matsumoto, H. Koinuma and Y. Nakato, *J. Phys. Chem. B.*, **2005**, *109*, 1648.
10 S. Yae, M. Kitagaki, T. Hagihara, Y. Miyoshi, H. Matsuda, B. A. Parkinson, Y. Nakato, *Electrochim. Acta*, **2001**, *47*, 345.
11 S. Takakusagi, K. Fukui, R. Tero, K. Asakura, Y. Iwasawa, *Langmuir*, **2010**, *26*, 16392.
12 S. Gan, Y. Liang, D.R. Baer, A.W. Grant, *Surf. Sci.* **2001**, 475, 159.
13 I.M. Tidswell, N.M. Markovic, P.N. Ross, *Phys. Rev. Lett.*, **1993**, *71*, 1601.
14 K. Wu, M. S. Zei, *Surf. Sci.*, **1998**, *415*, 212.
15 S. Mukherjee, B. Ramalingam, S. Gangopadhyay, *J. Mater. Chem A*, **2014**, *2*, 3954.
16 M. Heemeier, M. Frank, J. Libuda, K. Wolter, H. Kuhlenbeck, M. Baumer, H.J. Freund, *Catal. Lett.* **2000**, *68*, 19.
17 Z. Lodziana, J. K. Norskov, *J. Chem. Phys.* **2001**, *115*, 11261.
18 X. Tong, L. Benz, S. Chrétien, H. Metiu, M.T. Bowers, S.K. Buratto, *J. Phys. Chem. C*, **2010**, *114*, 3987.